

Article

Compact, Fast Cavity Ring-Down Spectroscopy Monitor for Simultaneous Measurement of Ozone and Nitrogen Dioxide in the Atmosphere

Xiaoyan Liu ¹, Zhijing Hu ¹, Hehe Tang ¹, Huijie Xue ¹, Yang Chen ^{2,*} and Renzhi Hu ^{3,*}¹ School of Pharmacy, Anhui Medical University, Hefei 230032, China² Department of Chemical Physics, University of Science and Technology of China, Hefei 230026, China³ Key Laboratory of Environment Optics and Technology, Anhui Institute of Optics and Fine Mechanics, Hefei Institutes of Physical Science, Chinese Academy of Sciences, Hefei 230031, China

* Correspondence: yangchen@ustc.edu.cn (Y.C.); rzhu@aiofm.ac.cn (R.H.)

Abstract: A sensitive, compact detector for the simultaneous measurement of O₃ and NO₂ is presented in this work. There are two channels in the detector, namely the O_x channel and the NO₂ channel. In the presence of excess NO, ambient O₃ is converted to NO₂ in the O_x measurement channel. In both channels, NO₂ is directly detected via cavity ring-down spectroscopy (CRDS) at 409 nm. At a 10 s integration time, the O_x and NO₂ channels have a 1σ precision of 14.5 and 13.5 pptv, respectively. The Allan deviation plot shows that the optimal sensitivity of O₃ and NO₂ occurs at an integration time of ~60 s, with values of 10.2 and 8.5 pptv, respectively. The accuracy is 6% for the O₃ channel and 5% for the NO₂ channel, and the largest uncertainty comes from the effective NO₂ absorption cross-section. Intercomparison of the NO₂ detection between the NO₂ and O_x channels shows good agreement within their uncertainties, with an absolute shift of 0.31 ppbv, a correlation coefficient of R² = 0.99 and a slope of 0.98. Further intercomparison for ambient O₃ measurement between the O₃/NO₂-CRDS developed in this work and a commercial UV O₃ monitor also shows excellent agreement, with linear regression slopes close to unity and an R² value of 0.99 for 1 min averaged data. The system was deployed to measure O₃ and NO₂ concentrations in Hefei, China, and the observation results show obvious diurnal variation characteristics. The successful deployment of the system has demonstrated that the instrument can provide a new method for retrieving fast variations in ambient O₃ and NO₂.

Keywords: CRDS; O₃; NO₂; simultaneous measurement; intercomparison

Citation: Liu, X.; Hu, Z.; Tang, H.; Xue, H.; Chen, Y.; Hu, R. Compact, Fast Cavity Ring-Down Spectroscopy Monitor for Simultaneous Measurement of Ozone and Nitrogen Dioxide in the Atmosphere. *Atmosphere* **2022**, *13*, 2106. <https://doi.org/10.3390/atmos13122106>

Academic Editor: Ole Hertel

Received: 15 November 2022

Accepted: 13 December 2022

Published: 15 December 2022

Publisher's Note: MDPI stays neutral with regard to jurisdictional claims in published maps and institutional affiliations.



Copyright: © 2022 by the authors. Licensee MDPI, Basel, Switzerland. This article is an open access article distributed under the terms and conditions of the Creative Commons Attribution (CC BY) license (<https://creativecommons.org/licenses/by/4.0/>).

1. Introduction

Ozone is a key atmospheric trace gas that is produced and transported in both the troposphere and stratosphere and influences atmospheric radiation and chemical processes. Ozone precursors come from natural and anthropogenic sources, such as lightning, vegetation, wildfires, and other types of biomass and fossil fuel combustion. In the troposphere, ozone is formed mainly through photochemical reactions of nitrogen oxides and volatile organic compounds, and has important effects on radiation forcing, gaseous photochemistry, and human, animal, and plant health [1,2]. It is the main source of OH free radicals and directly affects atmospheric chemical processes [3]. Tropospheric ozone is also a potent natural and anthropogenic greenhouse gas (IPCC, 2007). In view of the profound influence of ozone in the atmosphere, it is the most commonly measured trace gas in the atmosphere, which is very important in environmental monitoring.

Ozone's widely varying ambient mixing ratios, which range from parts per billion to parts per million, and its reactivity impose constraints on the sensitivity, dynamic range, and response rate necessary for an instrument making in-situ O₃ measurements.

Optical detection technology is widely used in the measurement of environmental trace gases [4–6]. A number of different techniques are commonly used for in-situ O₃ measurements in environmental research, including UV absorption [7], chemiluminescence [8], differential optical absorption spectroscopy (DOAS) [9], long path absorption photometry [10], and cavity-enhanced spectroscopy [11–13]. Because of its absoluteness, overall simplicity, and reliability, the UV absorption technology (UV-O₃) is the most widely used, especially in air quality monitoring networks. It uses 254 nm ultraviolet light to measure the concentration of O₃, which may be interfered with by volatile organic compounds (VOCs). The detection limit is about 1 ppbv (1 min) [14]. Chemiluminescence technology (NO-CL-O₃ technology) measures the chemiluminescence of the electron-excited state of NO₂ generated by the reaction of NO and O₃ to obtain the concentration of NO or O₃, and the detection limit can reach 0.01 ppbv. The technology requires a certain concentration of NO, a vacuum system, and must be calibrated to determine the relationship between the number of photons and the concentration of O₃. It has certain applicability, but it may be affected by changes in the atmospheric water vapor concentration [8]. Differential absorption spectroscopy (DOAS) has been applied to the monitoring of atmospheric ozone by Axelsson et al. [15]. Using a high-pressure xenon lamp as the light source, the average concentration of ozone in an absorption optical path of several hundred meters can be obtained by measuring the absorption spectrum in the range of 280–290 nm. Differential absorption spectroscopy has also played an important role in the monitoring of atmospheric conventional pollutants (O₃, NO₂, SO₂) in China.

A few comparative experiments have been conducted between UV-O₃ technology, NO-CL-O₃ technology, and DOAS technology in both the ambient atmosphere and the simulation chamber. Ryerson et al. conducted a comparative experiment of airborne O₃ observation and found that UV-O₃ technology was in good agreement with NO-CL-O₃ technology [16]. Williams et al. found that O₃ concentrations measured at an urban/industrial site and onboard a ship using UV-O₃ technology were consistent with those measured using NO-CL-O₃ technology and DOAS technology [17]. Spicer et al. found that the UV-O₃ technique was affected by the absorption of mercury vapor at 254 nm, and the deviation in ozone concentration measured per 1 pptv of mercury vapor was 1 ppbv. At the same time, Spicer et al. also found that the deviation between the conventional UV-O₃ monitor and the UV-O₃ monitor fitted with a water removal device was ± 4.1 ppbv during the smog season [18]. Ollison et al. found that in hot and humid weather, the deviation between the UV-O₃ monitor and NO-CL-O₃ monitor may be as high as 6 ppbv [19]. Leston et al. studied the interference of some aromatic compounds on the UV-O₃ monitor in the simulation chamber. In mixtures containing high concentrations of toluene and C8 aromatics (o-xylene, p-xylene, and ethylbenzene), the UV-O₃ monitor overestimated ozone by 15% and 38%, respectively [20].

The concentration of VOCs and other ozone precursors is very high in China, which poses a great challenge to the accurate measurement of ozone. At the same time, in situ measurements of ozone are often conducted from airborne platforms such as airplanes and balloons to describe the photochemical and dynamic processes of the atmospheric environment. High-time-resolution measurements are needed to observe changes in the ozone mixing ratio in small-scale atmospheric structures, such as power plants, biomass combustion, and the fine structure of stratospheric invasion into the troposphere.

In view of the high sensitivity and time resolution of the cavity ring-down spectroscopy (CRDS) technique, this study applies it to the detection of atmospheric O₃. This paper focuses on the accurate measurement of the quantitative conversion of O₃ to NO₂ using CRDS technology. The composition, performance, and possible measurement interference of the dual cavity ring-down system for measuring O_x (O₃ + NO₂) and NO₂ are further discussed. The system is applied to the actual measurement of O₃ and NO₂ in the ambient atmosphere, the measured results are compared with those measured using a UV-O₃ monitor, and the performance of the CRDS system is analyzed.

2. Experimental Section

2.1. Cavity Ring-Down Spectroscopy

The CRDS measurement principle, which has been described in a previous article [21], is mainly based on the analysis of the ring-down time of the multiple reflection of light in the ring-down cavity to obtain the concentration information of the gas. The concentration of the gas to be measured in the cavity can be obtained by the following equation:

$$[A] = \frac{R_L}{c\sigma} \left(\frac{1}{\tau} - \frac{1}{\tau_0} \right), \quad (1)$$

In Equation (1), $[A]$ and σ are the concentration and absorption cross-section of gas A, respectively, and c is the speed of light. R_L is the ratio of the ring-down cavity length to the single absorption optical path length of the gas in the cavity. τ_0 is the background ring-down time (when there is no gas A to be measured). τ is the ring-down time (including gas A to be measured). Therefore, when the absorption cross-section of NO_2 is known (it can be measured by the system τ and τ_0), the concentration of NO_2 can be calculated.

2.2. CRDS Instrument for NO_2 and O_3 Detection

As shown in Figure 1, the CRDS experimental system mainly includes a diode laser, timing control unit, optical isolator, diaphragm, two high-reflection cavities and two sets of high-sensitive data acquisition and processing systems. The diode laser (IQ μ , Power Technology Inc., USA) produces a continuous 409.05 nm laser with a power of 120 mW. The square wave signal with a modulation frequency of 2000 Hz and duty cycle of 50% is generated by the self-designed timing control unit to control the continuous optical diode laser and cause it to pulse the output. The laser switch response time is about 40 ns, which is far shorter than the ring-down time of the system. The laser passes through an optical isolator (IO-5-405-LP, Thorlabs) to prevent the light reflected by the high-reflection mirror from entering the diode laser and affecting the stability of the laser. After passing through a mirror, the laser is divided into two beams by a 50:50 beam splitter, each of which is directed into a ring-down cavity (along the axis of the high-reflection cavity) composed of two high-reflection mirrors (CRD Optics). Each high-reflection mirror is a 25.4 mm flat concave mirror with a curvature radius of 1 m, and the reflectivity calibrated by the manufacturer is 99.995%. To reduce the impact of the wall collision effect, perfluoroalkoxy (PFA) pipe is used to form a high-reflection cavity (cavity length: 750 mm) and air intake unit. To reduce pollution of the high-reflection mirror, high-purity N_2 is used to purge the lens to ensure the stability of the system. After the modulated pulse laser enters the high-reflection cavity, the output optical signal passes through a 10 nm band-pass filter (central wavelength: 405 nm) and is received by the photomultiplier tube (PMT), then is converted into an electrical signal. The signal is averaged and fitted on the computer through the acquisition card (PCI 6132, NI) with a sampling rate of 2.5 MHz controlled by LabVIEW, and the ring-down time is obtained. The pressure in the cavity is monitored in real time through the pressure sensor (ZJ-2Y, Reborn) at the outlet of the ring-down cavity.

The air inlet of the system is mainly composed of a three-way solenoid valve controlled by the timing unit, activated carbon adsorbent, MnO_2 adsorbent, and a pressure regulating valve. Once the atmosphere is sampled using the sampling pipe, the flow direction of the gas is controlled by the three-way solenoid valve. When the gas flow passes through the pressure-regulating valve, the ring-down chamber measures the ring-down time (containing absorbed NO_2 converted from NO_2 or O_3). When the gas flow passes through the activated carbon adsorbent and MnO_2 adsorbent (the activated carbon adsorbent will adsorb trace gases such as NO_2 and O_3 , and the MnO_2 adsorbent will remove any remaining O_3), the ring-down cavity measures the background ring-down time (measuring zero air). Through the timing control of the three-way solenoid valve, the ring-down time and the background ring-down time are each measured. The background ring-down time is

measured every 10 min to reduce the measurement error caused by small changes. The real-time concentration of NO₂ (or O_x) can be calculated according to Equation (1).

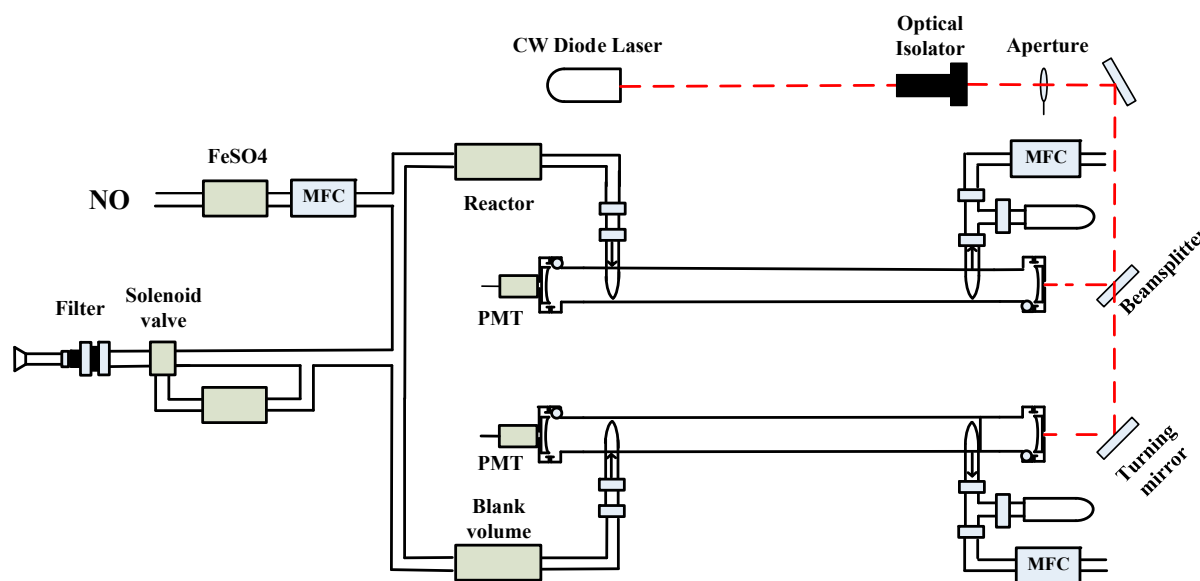


Figure 1. Schematic diagram of the CRDS–O_x/NO₂ system.

3. Results and Discussion

3.1. Effective NO₂ absorption cross-section

It is very important to determine the effective absorption cross-section of NO₂ for accurately quantifying the concentration of NO₂ (or O_x). In this study, the high-resolution absorption cross-section of NO₂ is convolved with the laser spectrum to obtain the effective absorption cross-section of the system. The diode laser manufacturer only provides a laser wavelength of 410.2 nm for continuous output, and NO₂ has a complex absorption structure in this spectral region. Thus, a more accurate laser wavelength and its half-height linewidth are needed to determine the absorption cross-section of NO₂. When the diode laser is externally modulated, its laser wavelength appears as a blue shift. In this system, the diode laser is pulse modulated using a square wave signal with a modulation frequency of 2000 Hz and duty cycle of 50%. The laser wavelength and linewidth of its output are measured using a grating spectrometer (SR303i, Andor). Figure 2 shows that the center wavelength of the modulated laser is 409.05 nm and the FWHM is 0.65 nm. In addition, the water vapor absorption spectrum [22] (as shown by the pink line in Figure 2) obtained from the HITRAN database shows that H₂O is not absorbed between 402 nm and 415 nm. The laser wavelength needs to be selected within this range to avoid absorption interference by H₂O. This improves the accuracy of the measurement, as there is no need to dry the sampled gas. Figure 2 also shows the absorption cross-section of NO₂ [23], and the effective absorption cross-section of the system obtained when convoluting it with the measured laser spectrum is $6.22 \times 10^{-19} \text{ cm}^2 \text{ molecule}^{-1}$. The stability of the laser wavelength was studied, and it is capable of maintaining the accuracy of the effective absorption cross-section of NO₂.

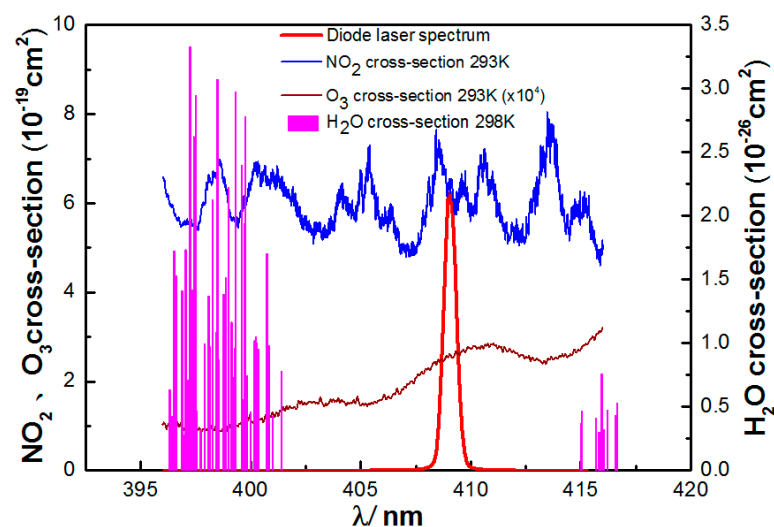


Figure 2. Absorption cross-section of NO_2 , O_3 , and water vapor and typical diode laser spectrum.

3.2. Zero Measurement

The background ring-down time (τ_0) must be measured regularly, considering the potential shift of τ_0 due to changes in temperature, pressure, mirror reflectance, and the stability of the cavity. The measured background ring-down time, measured by placing zero air without NO_2 directly into the sampling system, exhibits good stability. However, because of the extremely low water vapor content in the zero air, which changes the Rayleigh scattering of water vapor, there is still a certain error in the measurement of τ_0 . At the same time, owing to the need to carry zero air in the field measurement, the operation is not convenient. Therefore, in this system, an automatic switching air circuit was designed through the solenoid valve. Ambient air is directly introduced into the ring-down cavity after absorbing NO_2 through activated carbon to measure the background ring-down time. It has very good stability, and the standard deviation of the background ring-down time (time resolution of 1 s) is less than $0.02 \mu\text{s}$ within a 10 min interval. Since the absorption of water vapor by activated carbon is very small, the influence of the Rayleigh scattering change can be ignored. The adsorption effect of activated carbon was tested in the laboratory. In comparing new activated carbon and activated carbon used for 30 days, there was little difference in their adsorption effects. The background ring-down signal measured by the system is shown in Figure 3, where it is shown to have good single exponential characteristics, and thus the background ring-down time can be obtained via fitting.

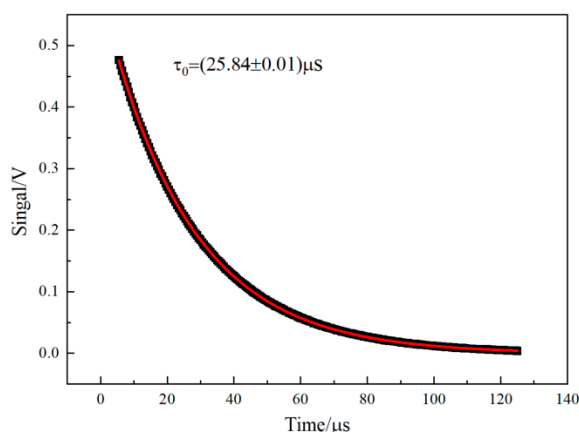


Figure 3. Cavity ring-down signal and fitting results.

3.3. O₃ conversion Efficiency

Real-time measurement of O₃ requires simultaneous measurement of two ring-down cavities. One ring-down cavity measures the concentration of O_x in real time, and the other ring-down cavity measures the concentration of NO₂ synchronously. The concentration of O₃ can be calculated via the differences between the measurement results of the two ring-down cavities. Therefore, the premise of accurately measuring O₃ concentration is to determine the conversion rate of O₃ to NO₂ according to the following reaction:



The reaction rate of (2) is $k = 3.0 \times 10^{-12} \exp(-1500 \text{ K}/T)$, that is, at 298 K, $k = 2 \times 10^{-14} \text{ cm}^3 \text{ molecule}^{-1} \text{ s}^{-1}$ [24]. NO cylinder gas (502 ppmv, Nanjing special gas) is injected into the sampling gas path through the solenoid valve, and its flow is controlled using a flowmeter. The sampling gas flow of the system is 2 L/min, and the reaction time of NO and O₃ in the sampling gas path is about 0.83 s. The relationship between the O₃ conversion rate and NO concentration measured in the laboratory is presented in Figure 4, where it is shown to have a very good single exponential relationship. In other words, reaction (2) can be regarded as a pseudo first-order reaction (i.e., NO is completely in excess). Specifically, when the concentration of NO is 10 ppmv, the conversion rate of O₃ is 98.6% in the sampling gas flow with an O₃ concentration of 220 ppbv. When measuring the atmospheric O₃ concentration, the difference between the O_x cavity and the NO₂ cavity is corrected using the conversion rate.

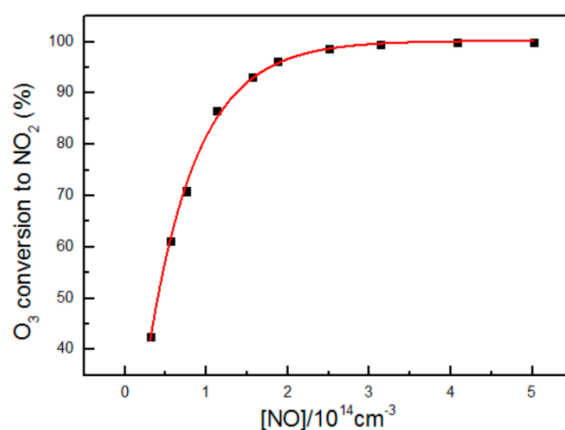


Figure 4. Conversion efficiency of 220 ppbv O₃ to NO₂ as a function of NO concentration.

3.4. Consistency of NO₂ Measurement

To accurately obtain the concentration of O₃, it is necessary to ensure that the measurement of NO₂ in the two ring-down cavities has very good consistency. During measurement of the actual ambient atmosphere, NO is not added to the sampling gas path, and the two ring-down cavities are both used to measure NO₂. The ambient atmospheric NO₂ concentration measured continuously for 39 h is shown in Figure 5. The measurement results of the two chambers are very consistent. The correlation analysis shows that the slope is 0.98 and the intercept is 0.31. The small difference between the measurements of the two ring-down cavities will be further corrected to achieve an accurate measurement of O₃ concentration.

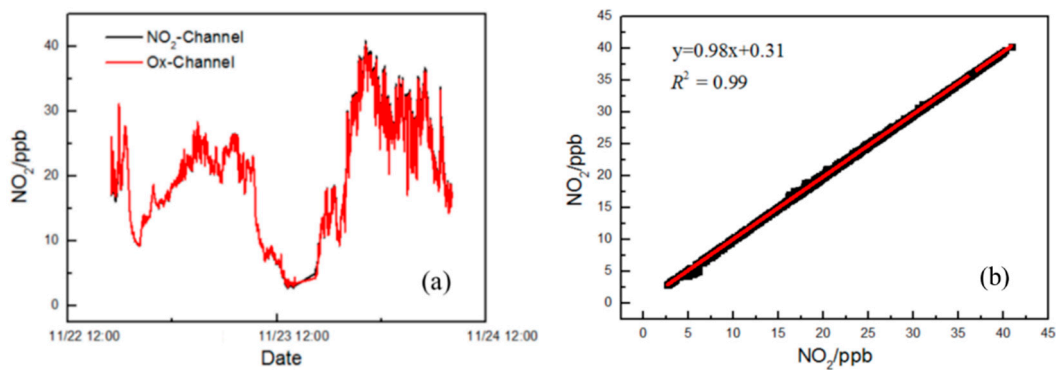


Figure 5. (a) Time series of ambient atmospheric NO₂ concentration sampled using the CRDS instrument in two channels. The time resolution is 1 s. (b) Correlation plot between the data from the two channels.

3.5. NO₂ and O₃ Detection Performance

The stability of the two ring-down cavities and the deviation of the measured results were investigated by directly measuring the ambient atmosphere after passing through the activated carbon adsorbent and MnO₂ adsorbent. Figure 6 shows the results of continuous measurement for 15 h, with a time resolution of 1 s. The measurement results of the NO₂ cavity are between −120 and 120 pptv and the measurement results of the O_x cavity range from −150 to 150 pptv (1 s).

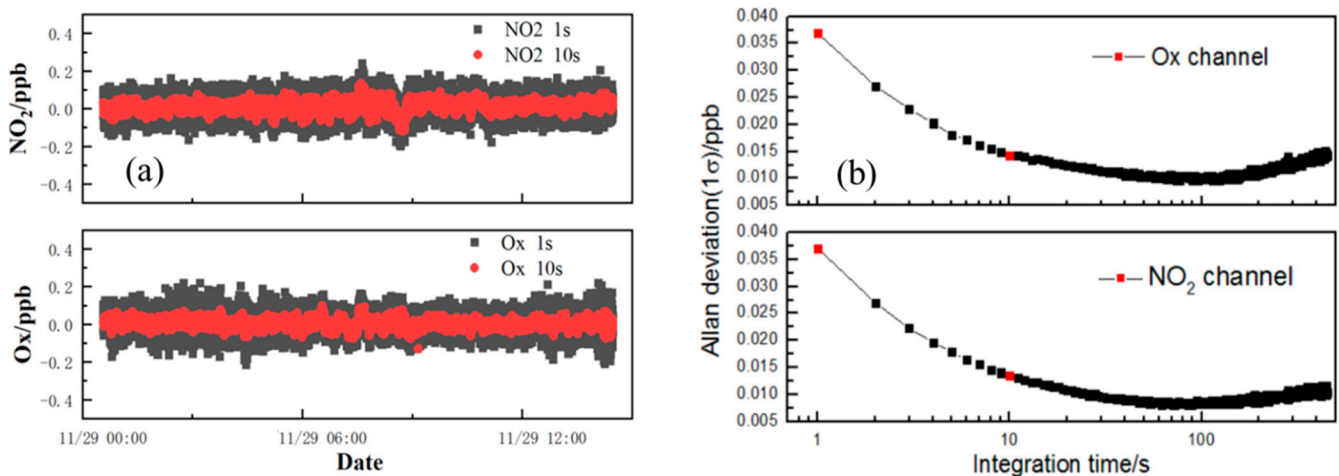


Figure 6. (a) Continuous time series measurement of ambient air after absorption by activated carbon, averaged to 1 s for the NO₂ and O_x channels (black dots); the red dots show the data averaged to 10 s. (b) Allan deviation plots for NO₂ concentration in two channels. The minimum value equals the optimum integration time.

The detection limit of the cavity ring-down system can be obtained by the following equation:

$$[O_x]_{\min} = \frac{R_L}{c\sigma} \frac{(\tau_0 - \tau)_{\min}}{\tau_0^2} = \frac{R_L}{c\sigma} \frac{\Delta\tau}{\tau_0^2} \cong \frac{R_L}{c\sigma} \frac{\sqrt{2}\sigma(\tau_0)}{\tau_0^2}, \quad (3)$$

where $[O_x]_{\min}$ represents the detection limit of the O_x gas in the system; $\Delta\tau$ indicates the stability of the background ring-down time, which is generally defined as $\sqrt{2}\sigma(\tau_0)$ [25]; and R_L is obtained by laboratory measurement, which is 1.09 in this system [25]. The minimum detection limits for the NO₂ and O_x channels are determined as 36.9 and 37.5 pptv, respectively, at an integration time of 1 s, which are close to the values obtained from the Allan variance analysis described below. Allan variance analysis was performed to

further explore the detection performance of the system, and the results are shown in Figure 6b. The detection limits are 13.5 and 14.5 pptv (10 s) for the NO₂ and O_x channels, respectively. The minima in the Allan plots indicate that the optimum average time for optimum detection performance is about 60 s. With a 60 s integration time, the detection limits are 8.5 and 10.2 pptv for the NO₂ and O_x channels, respectively, which are more suitable for measuring the background area.

A comparison of detection performance between this system and other O₃ instruments is presented in Table 1.

Table 1. Performance comparison of ozone instruments.

Method	Sensitivity	Time resolution	Reference
UV absorption	1 ppbv	1 s	[26]
UV absorption	0.4 ppbv	0.5 s	[27]
CEAS	31 pptv	1 s	[11]
CRDS	26 pptv	1 s	[13]
CEAS	8 ppbv	10 s	[28]
CEAS	1 ppbv	0.1 s	[12]
CRDS	14.5 pptv	10 s	This work

Considering that the error of the NO₂ absorption cross-section is about 4% [25], the measurement error of the R_L value is about 3%, and other errors (e.g., pressure, temperature) are about 1%, then the total uncertainty of NO₂ and O₃ measurement via CRDS is estimated to be 5% and 6%, respectively.

3.6. Assessment of O₃/NO₂-CRDS Measurement Accuracy

The accurate measurement of NO₂ was achieved based on cavity ring-down technology, but to determine the measurement accuracy of the O₃/NO₂-CRDS system, it was necessary to conduct a comparison of O₃ measurements in the laboratory. Ozone at a concentration of 500 ppbv was produced using an ozone generator, and two flowmeters were used to control the flows of ozone and N₂, resulting in an ozone concentration range of 20 to 200 ppbv. Because the concentration deviation of O₃ produced by the ozone generator is relatively large, and in addition there is a certain error associated with obtaining different concentrations of ozone via the dilution method, here the accuracy of the O₃/NO₂-CRDS measurement was determined by comparing to the measurement of an ozone analyzer. Specifically, the diluted O₃ was sampled through a sampling gas path and then divided between the O₃/NO₂-CRDS and ozone analyzer (Thermo Electron Scientific 49i) for synchronous detection. The measurement results are shown in Figure 7. The results of the two systems have good consistency, with a slope of 0.99, an intercept of only 0.48 ppbv, and a linear correlation of 0.99. The results show that O₃/NO₂-CRDS has good detection performance, and the calibration of the ozone conversion rate of the system is also very accurate. Furthermore, these results also indicate that this system is suitable for the monitoring of O₃ in the ambient atmosphere.

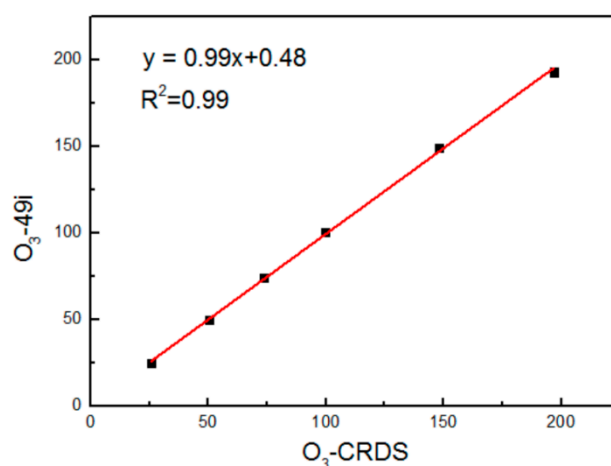


Figure 7. Correlation plot comparing O_3 measurements acquired by CRDS and the 49i ozone analyzer.

3.7. Field Measurement and Intercomparison

To further verify the field detection performance of the O_3/NO_2 -CRDS, the online measurement of ambient atmospheric O_3 and NO_2 was conducted at Hefei Science Island in November 2021. Science Island is located in the northwest suburb of Hefei, about 12 km away from the city center. The ambient air was sampled at the top of the laboratory building (28 m tall). A polytetrafluoroethylene (PTFE) filter with a pore size of $0.22 \mu\text{m}$ (Millipore, 47 mm diameter) was installed at the top of the sampling tube to remove particles that can cause large laser light scattering. The length of the PTFE tube (inner diameter 4.6 mm) from the sampling point to the cavity was 3 m. The ambient air was aspirated through the tube with a diaphragm pump (KNF, N86KNE) at a rate of 2 L min^{-1} . Figure 8 shows the results of the simultaneous measurement of ambient NO_2 and O_3 for 76 h. The NO_2 concentrations in the daytime are relatively lower than those in the nighttime. Photodissociation of NO_2 by sunlight and convective mixing in the boundary layer can account for the relatively low level of NO_2 in the daytime. The NO_2 photodissociation produces the $O(^3P)$ atom, which is followed by O_3 formation through the recombination reaction. Therefore, the concentration of ozone is high during the day and low at night. NO_2 and O_3 have obvious diurnal variation characteristics. To further explore the accuracy of the atmospheric O_3 measurement, the concentration of O_3 in the sample air was simultaneously measured with the ozone analyzer 49i (Figure 8, red line). The ozone concentrations measured using the O_3/NO_2 -CRDS and 49i exhibit very good consistency. The correlation analysis shows that the slope is 1, the intercept is -0.21 ppbv , and the linear correlation is 0.99. The O_3/NO_2 -CRDS system has better field detection ability. Compared with the ultraviolet absorption method (49i), it has a better detection limit and time resolution, and is more suitable for ground-based, vehicle-mounted, airborne, and other multi-platform applications.

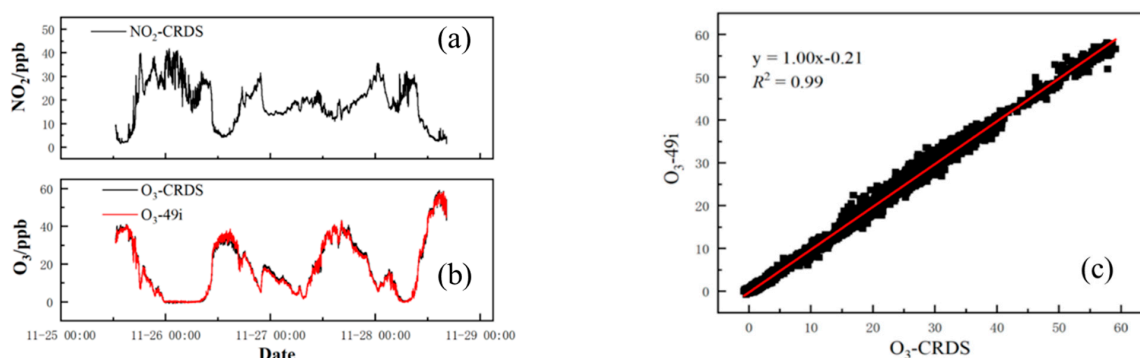


Figure 8. (a) NO_2 mixing ratios via CRDS (1 min average). (b) O_3 mixing ratios via CRDS and 49i (1 min average). (c) Scatter plots for the O_3 dataset from CRDS and the 49i ozone analyzer. The red lines illustrate the linear regression.

4. Conclusions

A cavity ring-down spectrometer with adequate selectivity and sensitivity for in situ simultaneous measurements of O₃ and NO₂ in the troposphere was developed. It offers accuracy comparable to commercial UV absorption instruments, but with substantially improved sensitivity and time response. The instrument described here demonstrates an accuracy of 6%, detection sensitivity of 14.5 pptv in ambient air after absorption by the activated carbon adsorbent and MnO₂ adsorbent, and a 10 s time resolution. The O₃/NO₂-CRDS instrument was compared in the laboratory and in the field with an 49i ozone analyzer under a variety of sampling conditions. The O₃/NO₂-CRDS and 49i O₃ measurements were highly correlated over wide concentration ranges of O₃ and were within the combined stated measurement uncertainties. The combination of simultaneous NO₂ and O₃ measurements offers additional advantages in convenience and accuracy over existing instruments. Commercial UV absorbance instruments do not offer NO₂ measurements. Thus, this instrument represents a simple, robust, and potentially low-cost method for these two related measurements.

Author Contributions: Conceptualization, X.L., Y.C. and R.H.; methodology, X.L. and R.H.; formal analysis, X.L. and R.H.; investigation, X.L., H.T., H.X. and Z.H.; resources, R.H.; writing—original draft preparation, X.L.; writing—review and editing, Y.C. and R.H.; All authors have read and agreed to the published version of the manuscript.

Funding: This research was funded by the National Natural Science Foundation of China (61905003, 62275250), the Natural Science Foundation of Anhui Province (No. 2008085J20), the Anhui Provincial Key R&D Program (2022107020022) and the National Key R&D Program of China (2017YFC0209401).

Institutional Review Board Statement: This is not applicable.

Informed Consent Statement: This is not applicable.

Data Availability Statement: The data used in this research are available upon request from the corresponding authors.

Acknowledgments: The authors would like to thank the anonymous reviewers for providing invaluable comments on the original manuscript.

Conflicts of Interest: The authors declare no conflict of interest.

References

1. Ashmore, M.R. Assessing the future global impacts of ozone on vegetation. *Plant Cell Environ.* **2005**, *28*, 949–964. [[CrossRef](#)]
2. Mudway, I.S.; Kelly, F.J. Ozone and the lung: A sensitive issue. *Mol. Asp. Med.* **2000**, *21*, 1–48. [[CrossRef](#)] [[PubMed](#)]
3. Levy, H. Normal atmosphere: Large radical and formaldehyde concentrations predicted. *Science* **1971**, *173*, 141–143. [[CrossRef](#)]
4. Qiao, S.D.; Sampaolo, A.; Patimisco, P.; Spagnolo, V.; Ma, Y.F. Ultra-highly sensitive HCl-LITES sensor based on a low-frequency quartz tuning fork and a fiber-coupled multi-pass cell. *Photoacoustics* **2022**, *27*, 100381. [[CrossRef](#)] [[PubMed](#)]
5. Wang, F.Y.; Hu, R.Z.; Chen, H.; Xie, P.H.; Wang, Y.H.; Li, Z.Y.; Jin, H.W.; Liu, J.G.; Liu, W.Q. Development of a field system for measurement of tropospheric OH radical using laser-induced fluorescence technique. *Opt. Express* **2019**, *27*, A419–A435. [[CrossRef](#)] [[PubMed](#)]
6. Liu, X.N.; Ma, Y.F. Tunable Diode Laser Absorption Spectroscopy Based Temperature Measurement with a Single Diode Laser Near 1.4 μ m. *Sensors* **2022**, *22*, 6095. [[CrossRef](#)]
7. Dunlea, E.J.; Herndon, S.C.; Nelson, D.D.; Volkamer, R.M.; Lamb, B.K.; Allwine, E.J.; Grutter, M.; Ramos Villegas, C.R.; Marquez, C.; Blanco, S.; et al. Technical note: Evaluation of standard ultraviolet absorption ozone monitors in a polluted urban environment. *Atmos. Chem. Phys.* **2006**, *6*, 3163–3180. [[CrossRef](#)]
8. Ridley, B.A.; Grahek, F.E.; Walega, J.G. A small, high-sensitivity, medium-response ozone detector suitable for measurements from light aircraft. *J. Atmos. Oceanic Technol.* **1992**, *9*, 142–148. [[CrossRef](#)]
9. Li, Y.L.; Zhang, X.X.; Li, X.; Cui, Z.L.; Xiao, H. Detection of Ozone and Nitric Oxide in Decomposition Products of Air-Insulated Switchgear Using Ultraviolet Differential Optical Absorption Spectroscopy (UV-DOAS). *Appl. Spectrosc.* **2018**, *72*, 1244–1251. [[CrossRef](#)]
10. Peters, S.; Bejan, I.; Kurtenbach, R.; Liedtke, S.; Villena, G.; Wiesen, P.; Kleffmann, J. Development of a new LOPAP instrument for the detection of O₃ in the atmosphere. *Atmos. Environ.* **2013**, *67*, 112–119. [[CrossRef](#)]

11. Hannun, R.A.; Swanson, A.K.; Bailey, S.A.; Hanisco, T.F.; Bui, T.P.; Bourgeois, I.; Peischl, J.; Ryerson, T.B. A cavity-enhanced ultraviolet absorption instrument for high-precision, fast-time-response ozone measurements. *Atmos. Meas. Tech.* **2020**, *13*, 6877–6887. [[CrossRef](#)]
12. Gomez, A.L.; Rosen, E.P. Fast response cavity enhanced ozone monitor. *Atmos. Meas. Tech.* **2013**, *6*, 487–494. [[CrossRef](#)]
13. Washenfelder, R.A.; Wagner, N.L.; Dubé, W.P.; Brown, S.S. Measurement of Atmospheric Ozone by Cavity Ring-down Spectroscopy. *Environ. Sci. Technol.* **2011**, *45*, 2938–2944. [[CrossRef](#)]
14. Clemitshaw, K.C. A review of instrumentation and measurement techniques for ground-based and airborne field studies of gas-phase tropospheric chemistry. *Crit. Rev. Environ. Sci. Technol.* **2004**, *34*, 1–108. [[CrossRef](#)]
15. Axelsson, H.; Edner, H.; Galle, B.; Ragnarson, P.; Rudin, M. Differential optical-absorption spectroscopy (DOAS) measurements of ozone in the 280–290 nm wavelength region. *Appl. Spectrosc.* **1990**, *44*, 1654–1658. [[CrossRef](#)]
16. Ryerson, T.B.; Buhr, M.P.; Frost, G.J.; Goldan, P.D.; Holloway, J.S.; Hübler, G.; Jobson, B.T.; Kuster, W.C.; McKeen, S.A.; Parrish, D.D.; et al. Emissions lifetimes and ozone formation in power plant plumes. *J. Geophys. Res. Atmos.* **1998**, *103*, 22569–22583. [[CrossRef](#)]
17. Williams, E.J.; Fehsenfeld, F.C.; Jobson, B.T.; Kuster, W.C.; Goldan, P.D.; Stutz, J.; Mcclenny, W.A. Comparison of Ultraviolet Absorbance, Chemiluminescence, and DOAS Instruments for Ambient Ozone Monitoring. *Environ. Sci. Technol.* **2006**, *40*, 5755–5762.
18. Spicer, C.W.; Joseph, D.W.; Ollison, W.M. A Re-Examination of ambient air ozone monitor interferences. *J. Air Waste Manag. Assoc.* **2010**, *60*, 1353–1364. [[CrossRef](#)]
19. Ollison, W.M.; Crow, W.; Spicer, C.W. Field testing of new-technology ambient air ozone monitors. *J. Air Waste Manag. Assoc.* **2013**, *63*, 855–863. [[CrossRef](#)] [[PubMed](#)]
20. Leston, A.R.; Ollison, W.M.; Spicer, C.W.; Satola, J. Potential interference bias in ozone standard compliance monitoring. *J. Air Waste Manag. Assoc.* **2005**, *55*, 1464–1472. [[CrossRef](#)]
21. Li, Z.Y.; Hu, R.Z.; Xie, P.H.; Chen, H.; Wu, S.Y.; Wang, F.Y.; Wang, Y.H.; Ling, L.Y.; Liu, J.G.; Liu, W.Q. Development of a portable cavity ring down spectroscopy instrument for simultaneous, in situ measurement of NO₃ and N₂O₅. *Opt. Express* **2018**, *26*, A433–A449. [[CrossRef](#)] [[PubMed](#)]
22. Rothman, L.S.; Gordon, I.E.; Barber, R.J.; Dothe, H.; Gamache, R.R.; Goldman, A.; Perevalov, V.I.; Tashkun, S.A.; Tennyson, J. HITEMP, the high-temperature molecular spectroscopic database. *J. Quant. Spectrosc. Radiat. Transf.* **2010**, *111*, 2139–2150. [[CrossRef](#)]
23. Voigt, S.; Orphal, J.; Burrows, J.P. The temperature and pressure dependence of the absorption cross-sections of NO₂ in the 250–800 nm region measured by Fourier-transform spectroscopy. *J. Photochem. Photobiol. A Chem.* **2002**, *149*, 1–7. [[CrossRef](#)]
24. Sander, S.P.; Friedl, R.R.; Ravishankara, A.R.; Golden, D.M.; Kolb, C.E.; Kurylo, M.J.; Molina, M.J.; Moortgat, G.K.; Keller-Rudek, H.; Finlayson-Pitts, B.J.; et al. *Chemical Kinetics and Photochemical Data for Use in Atmospheric Studies*; NASA Jet Propulsion Laboratory: Pasadena, CA, USA, 2006.
25. Li, Z.Y.; Hu, R.Z.; Xie, P.H.; Chen, H.; Liu, X.Y.; Liang, S.X.; Wang, D.; Wang, F.Y.; Wang, Y.H.; Lin, C.; et al. Simultaneous measurement of NO and NO₂ by a dual-channel cavity ring-down spectroscopy technique. *Atmos. Meas. Tech.* **2019**, *12*, 3223–3236. [[CrossRef](#)]
26. Kalnajs, L.E.; Avallone, L.M. A Novel Lightweight Low-Power Dual-Beam Ozone Photometer Utilizing Solid-State Optoelectronics. *J. Atmos. Ocean. Technol.* **2009**, *27*, 869–880. [[CrossRef](#)]
27. Gao, R.S.; Ballard, J.; Watts, L.A.; Thornberry, T.D.; Ciciora, S.J.; McLaughlin, R.J.; Fahey, D.W. A compact, fast UV photometer for measurement of ozone from research aircraft. *Atmos. Meas. Tech.* **2012**, *5*, 2201–2210. [[CrossRef](#)]
28. Darby, S.B.; Smith, P.D.; Venables, D.S. Cavity-enhanced absorption using an atomic line source: Application to deep-UV measurements. *Analyst* **2012**, *137*, 2318–2321. [[CrossRef](#)]